

Simulation and Characterization of Microdilution Chip

Nurhaslinda binti Mazlan¹, Intan Sue Liana Abdul Hamid^{1*}

¹Faculty of Electrical and Electronic Engineering,
Universiti Tun Hussein Onn Malaysia, 86400 Parit Raja, Johor, MALAYSIA

*Corresponding Author Designation

DOI: <https://doi.org/10.30880/eeee.2021.02.01.001>

Received 09 February 2021; Accepted 12 April 2021; Available online 30 April 2021

Abstract: Extraction liquid methods is currently being applied in various of fields such as biochemical engineering, biochemistry, and biology applications. In this work, a microdiluter chip is designed and simulated for simultaneously carrying out multiple solution with different concentrations. There are four set solutes used in this project which are water/heptane, water/ethanol, water/glycerol, and water/diethyl ether. The COMSOL software used in this work produce a precise result of microdiluter that is able to produce 30%, 70%, 80%, 90% and 100% of dilution.

Keywords: Concentration, Microdilution, Laminar, Mixing

1. Introduction

Microfluidics is a system that can process small quantities of fluids by using tiny channels having dimensions at the micro- scale – typically tens to hundreds of micrometers [1]. Although in the nascent stage, microfluidics is rapidly emerging as a breakthrough technology that finds applications in diverse fields ranging from biology and chemistry to information technology and optics [2]. The systems are developed and analyzed through COMSOL Multiphysics software. On the 2D and 3D models, the suggested physics modules were added to assist the process of dilution of fluids [3]. Lab on a chip is very convenient for microfluidic devices. It is applicable to carry out functions such as diluting, mixing, and splitting of fluids [4]. This project focuses on the simulation and characterization of microdilution chips. Generally, the definition of microdilution is the combination of a small volume of the material that is desired to be diluted with a volume of diluent. Dilution consists of only two input reagents (commonly known as sample and buffer) are mixed in a desired volumetric ratio [5]. The project's purpose is to separate the concentration of a chemical solution by infusing a volume of distilled water combine with an amount of chemical solution to find the concentration of a solution by using the dilution process. It consists of two-tier input would be the distilled water and solvent, both solutions are flowed through four flow channels of microfluidic then mix to produce the concentration obtain through the four outlets of the microfluidic device [6].

Microdilution plays a significant role in the bioanalysis process. Normally, the microdilution device enables serial dilutions to produce a high volume of reagent in multiple concentration gradients by using

*Corresponding author: liana@uthm.edu.my

2021 UTHM Publisher. All rights reserved.

publisher.uthm.edu.my/periodicals/index.php/eeee

the dilution technique. The goal of designed a microdilution chip is to avoid waste and to obtain quantitative data. The functional performance of passively operated diluting microfluidics is sensitive with respect to the channel network dimensions, the precision of the simulation as well as the pressure applied because the whole network is linked together. The local and global changes in hydrodynamic resistance caused by dilute in particular make the task of developing a robust microfluidic design challenging as the designer has to consider plenty of interdependencies that all affect the intended behavior. Normally, its functionality is validated after the design by producing a prototype and testing it with physical experiments. When the interface is not implemented as expected, the designer must go back, revise the design, and repeat the manufacturing and experiments as well. This current design process is based on multiple refining and design testing iterations and produces high costs.

2. Materials and Methods

COMSOL Multiphysics v5.5 is used in handling this project. In the simulation process, the method is used to obtain an approximate solution by using numerical simulation. The discretization method used approximates the differential equations through a system algebraic equation, which can be solved on a computer [12]. There are three sequence phases before COMSOL Multiphysics produces results. The begins with the development of microdilution chip, sub-domain setup, boundary setup, mesh generation, simulation to post output processing. The phases are classified under pre-processing, processing, and post-processing as shown in Figure 1 below.

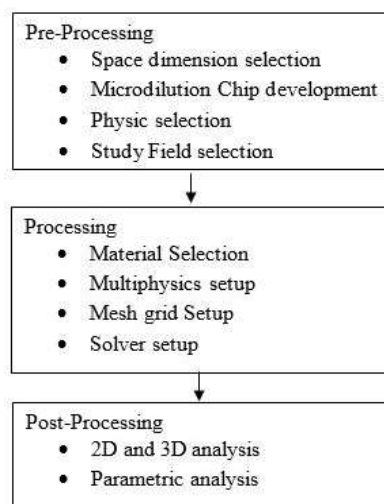


Figure 1: COMSOL Multiphysics phase sequences

The type of design preferred in this project known as tree design shape. Through research work, tree shape network is a typical practice of pressure-driven systems. For easy understanding, this shape is usually considered as an analogy to the electronic circuit as plotted in Figure 2. Where the pressure drop ΔP , volumetric flow rate Q , and hydraulic resistance R correspond to the voltage drop, current and electric resistance respectively. Analogous to Ohm's law, the Hagen – Poiseuille's law $\Delta P = RQ$ can be simplified. When the pressure drop and channel cross-section of each stage are the same, the hydrodynamic resistance of a channel is proportional to its length R directly proportional to length (L) [13]. Few parameters that must be considered before proceeding to the design process. Which is the diameter of inlets and outlets, length of the channel, diameter between each other for inlets and outlets, the width of the channel.

Figure 3 below shows the technical dimension of microfluidic dilute designed consists of two-port inlets and each with a diameter of $3.0 \mu\text{m}$ width and high. The diameter of each of the four-port outlets is $3.0 \mu\text{m}$ width and high. The total length of microdilution is $44.0 \mu\text{m}$. The width of the microdilution is around $21.0 \mu\text{m}$, and the length of the channel is $12 \mu\text{m}$. In terms of, T-junction should be short to

provide low resistance so that, the performance of fluid smooth to flow via a channel with high performance [18]. The depth of microdiluter channel is $1\mu\text{m}$. Meanwhile, the width of the channel is set to $1\mu\text{m}$, to ensure the performance of dilution in high-performance conditions. The three dimensional view of the microdiluter is described in Figure 4.

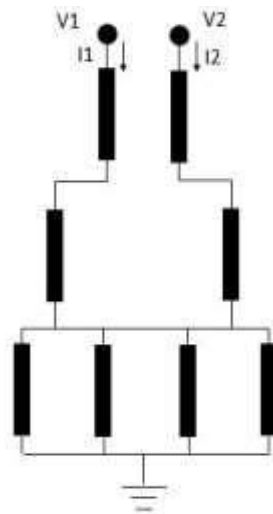


Figure 2: Electronic Circuit Plotted [13]

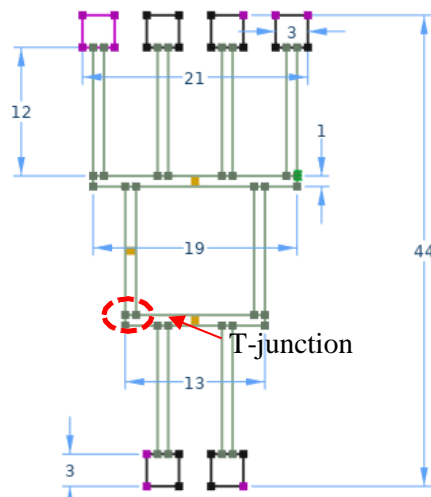


Figure 3: Technical dimension of microdilution design produced in COMSOL Multiphysics version 5.5

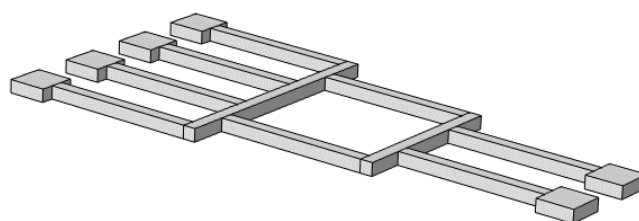


Figure 4: Tilt view of 3D microdilution design produced in COMSOL Multiphysics

3. Results and Discussion

The discussion will focus on the analysis of four different solutions by using microdilution chip design. The method is the diluting analysis according to the changes of color intensity. The output each of solution is analyzed in terms of percentage dilution occurred and the potential model to produce accurate data. Therefore, concentration surface is used to analyze the percentage dilution of solute while standard deviation concentration is used for quantifying the level of accuracy data occurred. The result analysis each of solute is then compared and discussed in the last section.

3.1 Results

The changes of color intensity for concentration profile microdilution chip for glycerol/water solute shown in Figure 5 the red color and blue color indicate that there are two fluids involved. The green color indicates the complete diluting which results in 0.5mol/m^3 in the concentration of the solutes. The red color at one inlet with a concentration of 1 mol/m^3 and blue color on the other inlet with a concentration of 0 mol/m^3 were spread towards microdilution chip.

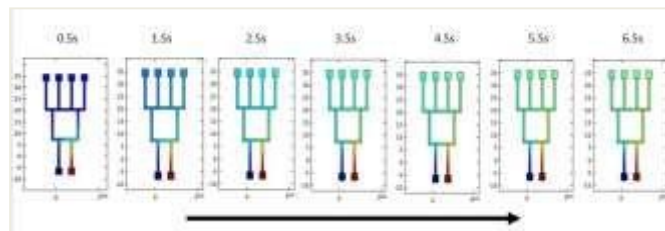


Figure 5: The changes of color intensity for concentration profile microdilution chip for glycerol/water solute

3.2 Dilution percentage analysis

Four sets of solutions were simulated and the results presented below are reviewed by the difference value of percentage dilution occurred each of outlets and standard deviation concentration. The performance of diluting each solute and the level of data precision of the device was characterized by determining the changes of color intensity. Figure 6, 7, 8 and 9 below shows the different values of percentage dilution that occurred for each outlet at complete diluting, for each set of mixed solutions. The detail percentage of dilution for each set is as listed in Table 1, 2, 3 and 4.

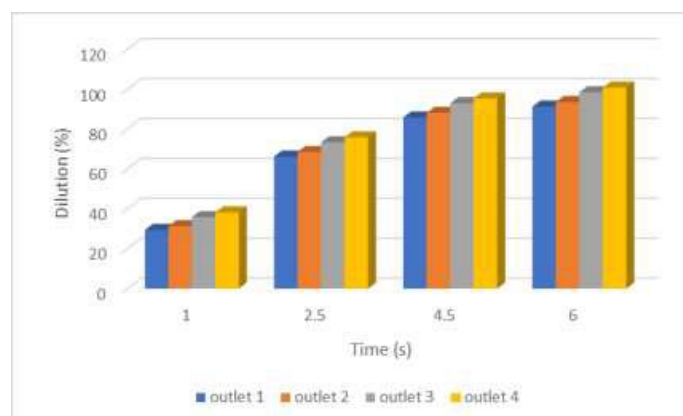


Figure 6: Dilution performance of Water/Heptane solute

Table 1: Percentage of dilution Water/Heptane solute (%)

	1(s)	2.5(s)	4.5(s)	6(s)
outlet 1	29.46	66.26	85.82	91.26
outlet 2	31.34	68.50	88.14	93.60
outlet 3	35.86	73.36	92.98	98.44
outlet 4	38.24	75.84	95.36	100.8

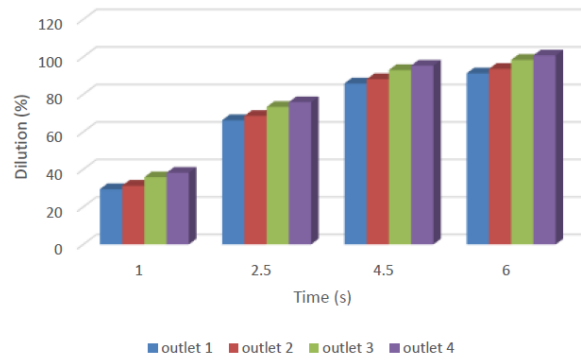


Figure 7: Dilution performance of Water/Ether solute

Table 2: Percentage of dilution Water/Ether solute (%)

	1(s)	2.5(s)	4.5(s)	6(s)
outlet 1	29.44	66.26	85.82	91.26
outlet 2	31.32	68.52	88.14	93.60
outlet 3	35.86	73.36	92.98	98.44
outlet 4	38.22	75.84	95.38	100.8

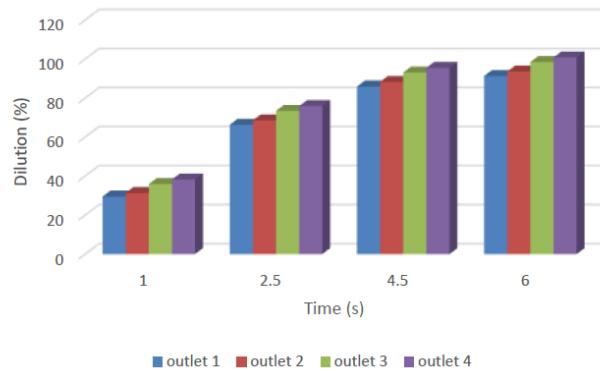


Figure 8: Dilution performance of Water/Glycerol solute

Table 3: Percentage of dilution Water/Glycerol solute (%)

	1(s)	2.5(s)	4.5(s)	6(s)
outlet 1	29.46	66.26	85.88	91.22
outlet 2	31.34	68.52	88.20	93.56
outlet 3	35.86	73.38	93.04	98.40
outlet 4	38.24	75.84	95.44	100.76

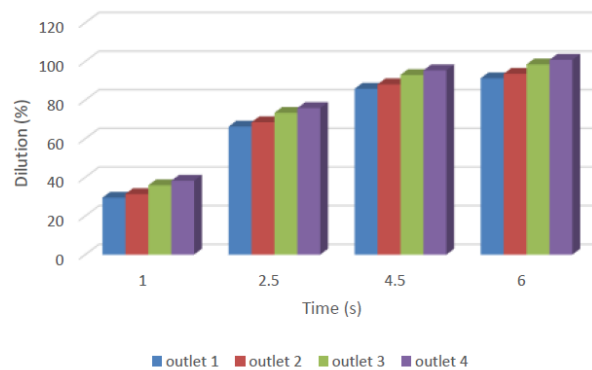


Figure 9: Dilution performance of Water/Ethanol solute

Table 4: Percentage of dilution Water/Ethanol solute (%)

	1(s)	2.5(s)	4.5(s)	6(s)
outlet 1	29.46	66.24	85.80	91.26
outlet 2	31.34	68.50	88.12	93.60
outlet 3	35.86	73.36	92.96	98.44
outlet 4	38.24	75.82	95.36	100.80

According to Figure 6-9, each of solute has produced linearity of dilution. The significant change value occurred at each time. Four types of fluids and water have flowed through devices at a combined flow rate of $1.7 \times 10^{-11} \text{ m}^3\text{s}^{-1}$. This value of flowrate is preferred because it represents the most likely flow rate that will be used with future cell studies it is fast enough to provide sufficient nutrients and remove waste, yet slow enough to not excessively shear cells. The resulting dilutions were close to the actual values. The greatest discrepancy occurred at the variety levels, which had normalized concentrations of 29.46%, 68.50%, 88.12%, 91.26%, and 100.8% for 30%, 70%, 90% and 100% values.

3.3 Standard deviation for concentration

Figure 10 shows the summarize value of standard deviation for four set of solutions. Based on the result obtained of four different solutes, the standard deviation for each solution in each dilution channel, the maximum standard deviation was $\pm 1.8 \times 10^{-5}$ while the minimum was $\pm 1.2 \times 10^{-5}$. The level of precision shows the data obtained still in high precision categorization. Therefore, to improve the stability and accuracy of the molecular gradient, the number of splitting stages of the tree shapes network needs to be increased.

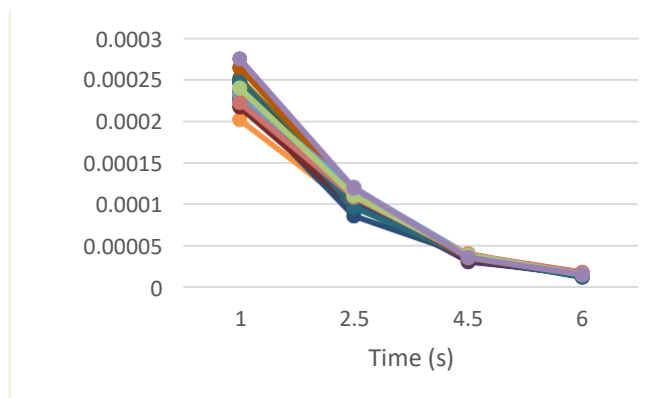


Figure 10: Standard Deviation at outlet for each solute

4. Conclusion

Overall, in this project, the microdilution chip design is successfully developed according to specific dimensions in two and three-dimensional. Based on the result analysis showed the characteristic of the device is capable of generating various percentage dilutions. The higher efficiency of the device was demonstrated by characterizing dilution linearity with one flow rate multiple times. Even though the precision is slightly unstable, the data obtained is close to 0 value. It means this device has the potential to produce high accuracy data. Therefore, Further research with various forms of design can be done to improve the level accuracy data with increase the number of splitting stages of the tree shape network.

Acknowledgement

. The author would like to thanks the Faculty of Electrical and Electronic Engineering, Universiti Tun Hussein Onn Malaysia for the facilities especially Mechatronic Laboratory that has been provided to complete this project and for its support.

References

- [1] Elshikh, M., Ahmed, S., Funston, S., Dunlop, P., McGaw, M., Marchant, R., & Banat, I. M. (2016). Resazurin-based 96-well plate microdilution method for the determination of minimum inhibitory concentration of biosurfactants. *Biotechnology letters*, 38(6), 1015- 1019.
- [2] Helios, K., Maniak, H., Sowa, M., Zierkiewicz, W., Wąsińska-Katwa, M., Giurg, M., ... & Krauze, K. (2017). Silver (I) complex with 2-amino-4, 4 α -dihydro- 4 α , 7-dimethyl-3 H-phenoxazin-3-one (Phx-1) ligand: crystal structure, vibrational spectra and biological studies. *Journal of Coordination Chemistry*, 70(20), 3471-3487.
- [3] Lin, Y., Gao, C., Gritsenko, D., Zhou, R., & Xu, J. (2018). Soft lithography based on photolithography and two-photon polymerization. *Microfluidics and Nanofluidics*, 22(9).
- [4] M. Trebbin, K. Kruger, D. DePonte, S. V. Roth, H. N. Chapman, & S. Forster, "Microfluidic liquid jet system with compatibility for atmospheric and high-vacuum conditions," *Lab on a Chip*, vol.14, pp. 1733-1745, 2014.
- [5] Bhattacharjee, S., Poddar, S., Roy, S., Huang, J. D., & Bhattacharya, B. B. (2016). Dilution and mixing algorithms for flow-based microfluidic biochips. *IEEE Transactions on Computer-Aided Design of Integrated Circuits and Systems*, 36(4), 614-627.
- [6] Connor, N. (2019, June 03). What is Laminar Flow - Viscous Flow - Definition. Retrieved October 19, 2020, from <https://www.thermal-engineering.org/what-is-laminar-flow-viscous-flow-definition/>.

- [7] Sundra, S., Soon, C. F., Zainal, N., Tee, K. S., Ahmad, N., & Gan, S. H. (2017). The Effects of Micromixing Two Solutions of Two Concentrations in a Two Tier PDMS Micromixer. IOP Conference Series: Materials Science and Engineering, 226, 012121.
- [8] Faustino, V., Catarino, S. O., Lima, R., & Minas, G. (2016). Biomedical microfluidic devices by using low- cost fabrication techniques: A review. Journal of biomechanics, 49(11), 2280-2292.
- [9] Onlaor, K., Thiawawong, T., & Tunhoo, B. (2016). Bi- stable switching behaviors of ITO/EVA:ZnO NPs/ITO transparent memory devices fabricated using a thermal roll lamination technique. Organic Electronics, 31, 19– 24.
- [10] Moumen, A. E., Tarfaoui, M., & Lafdi, K. (2019). Modelling of the temperature and residual stress fields during 3D printing of polymer composites. The International Journal of Advanced Manufacturing Technology, 104(5-8), 1661–1676.
- [11] Gale, B., Jafek, A., Lambert, C., Goenner, B., Moghimifam, H., Nze, U., & Kamarapu, S. (2018). A Review of Current Methods in Microfluidic Device Fabrication and Future Commercialization Prospects.
- [12] Roussel, N., Spangenberg, J., Wallevik, J., & Wolfs, R. (2020). Numerical simulations of concrete processing: from standard formative casting to additive manufacturing. Cement and Concrete Research, 135, 106075.
- [13] Vasilakis, N., Papadimitriou, K., Morgan, H., & Prodromakis, T. (2019). Modular Pressure and Flow Rate-Balanced Microfluidic Serial Dilution Networks for Miniaturised Point-of-Care Diagnostic Platforms. Sensors, 19(4), 911.
- [14] Vasilakis, N., Papadimitriou, K. I., Morgan, H., & Prodromakis, T. (2018). Novel modular pressure and flow rate balanced microfluidic serial dilution networks on printed circuit boards: Designs, Simulations and Fabrication. bioRxiv, 270124
- [15] Kim, D. N. H., Kim, K. T., Kim, C., Teitell, M. A., & Zangle, T. A. (2017). Soft lithography fabrication of index-matched microfluidic devices for reducing artifacts in fluorescence and quantitative phase imaging. Microfluidics and Nanofluidics, 22(1).
- [16] Giorgi, G., Gomes, R. P., Henriques, J. C., Gato, L. M., Bracco, G., & Mattiazzo, G. (2020). Detecting parametric resonance in a floating oscillating water column device for wave energy conversion: Numerical simulations and validation with physical model tests. Applied Energy, 276, 115421.
- [17] Gale, B., Jafek, A., Lambert, C., Goenner, B., Moghimifam, H., Nze, U., & Kamarapu, S. (2018). A Review of Current Methods in Microfluidic Device Fabrication and Future Commercialization Prospects. Inventions, 3(3), 60.
- [18] Sundra, S., Soon, C. F., Zainal, N., Tee, K. S., & Gan, S.H. (2016). The effects of flow rates to the concentration gradients in a passive micromixer low flow rate provides linear dilution of fluids. 2016 IEEE EMBS Conference on Biomedical Engineering and Sciences (IECBES).
- [19] Vasilakis, N., Papadimitriou, K., Morgan, H., & Prodromakis, T. (2019). Modular Pressure and Flow Rate-Balanced Microfluidic Serial Dilution Networks for Miniaturised Point-of-Care Diagnostic Platforms. Sensors, 19(4), 911.
- [20] Mukherjee, P., Nebuloni, F., Gao, H., Zhou, J., & Papautsky, I. (2019). Rapid Prototyping of Soft Lithography Masters for Microfluidic Devices Using Dry Film Photoresist in a Non-Cleanroom Setting. Micromachines, 10(3), 192.

- [21] Sala-Jarque, J., Mesquida-Veny, F., Badiola-Mateos, M., Samitier, J., Hervera, A., & del Río, J. A. (2020). Neuromuscular Activity Induces Paracrine Signaling and Triggers Axonal Regrowth after Injury in Microfluidic Lab-On-Chip Devices. *Cells*, 9(2), 302.
- [22] Sundra, S., Soon, C. F., Mahmud, F., Zainal, N., & Tee, K. S. (2017). Short Review on Techniques and Materials used for Microfluidic Device Fabrication. *proceeding of science, engineering & nanotechnology*, 15, 49.
- [23] Walker, G. M., Monteiro-Riviere, N., Rouse, J., & O'Neill, A. T. (2007). A linear dilution microfluidic device for cytotoxicity assays. *Lab on a Chip*, 7(2), 226- 232